Materials Chemistry and Physics 271 (2021) 124897

Contents lists available at ScienceDirect

Materials Chemistry and Physics

journal homepage: www.elsevier.com/locate/matchemphys

Half-metallicity in Fe_2MnSi and Mn_2FeSi heusler compounds: A comparative *ab initio* study

Oksana N. Draganyuk, Vyacheslav S. Zhandun *, Natalia G. Zamkova

Kirensky Institute of Physics - Federal Research Center "Krasnoyarsk Science Centre, Siberian Branch of the Russian Academy of Sciences, 660036, Krasnoyarsk, Russia

HIGHLIGHTS

- The properties of Heusler alloys is analyzed in terms of the local environment.
- The width of the half-metal bandgap is determined by the behavior of t2g electronic states.
- The pressure dependence of the magnetic and electronic properties were studied.

ARTICLE INFO

Keywords:
ab initio calculations
Heusler alloys
Magnetic properties
Half-metal
Pressure dependence

ABSTRACT

First-principles calculations of the structural, electronic, and magnetic properties of full-Heusler compounds Fe_2MnSi and Mn_2FeSi in regular $L2_1$ and inverse XA structures have been performed using density functional theory (DFT) within generalized gradient approximation (GGA) and SCAN functionals. All compounds indicate half-metallic properties with the minority spin bandgap. The causes for the appearance of half-metallic bandgap and the difference in the electronic and magnetic properties of Heusler compounds were studied and analyzed in terms of the local environment. It is shown, that the half-metallic bandgap determines by the behavior of the t_{2g}-electrons of A- and *C*-sites atoms. The behavior of the compounds under pressure was also considered. The high sensitivity of the magnetic moments on atoms A, C and the bandgap to pressure is discussed. The transition from regular to inverse structure is predicted at the negative pressure.

1. Introduction

The Heusler alloys with FCC- structure, draw great attention due to their possible application in microelectronic and spintronics. Some of such compounds are half-metal with 100%-spin polarization and high structural stability [1]. The structures, electronic and magnetic properties of many Heusler compounds have been earlier studied by first-principles DFT-based calculations [1–10] and experimental methods [11–13,18,19]. Full Heusler alloys crystallize within two possible structures: $L2_1$ (symmetry space group $Fm\underline{3}m$) and XA (symmetry space group $F\underline{4}3m$). Interest in these compounds is not the least because the properties of full Heusler alloys are strongly dependent on their structure and composition.

The effect of the composition on the band structure has been described through the example of $Fe_2Ti_{1-x}Mn_xAl$ Heusler alloys [4]. Fe_2TiAl is shown to be a metal compound in the $L2_1$ structure, but increasing the amount of Mn results in the appearance of a bandgap at 0.75% of Mn. The full-Heusler compounds Fe_2MnX and Mn_2FeX (X = Al, Si) in regular ($L2_1$) and inverse (XA) structures have been investigated by DFT + GGA methods in several works [2,15,16]. Ferromagnetic Fe_2MnSi and ferrimagnetic Fe_2MnAl [2] have indicated half-metallic behavior with vanishing electronic density of states for minority spin at the Fermi level in Cu_2MnAl-type $L2_1$ structure. The results of the first-principle calculations [2] are confirmed by the X-ray diffraction analysis [11,12] showing that Fe_2MnSi and Fe_2MnAl have $L2_1$ structures. The electrical and thermoelectric properties of these compounds have been considered by two-current conduction and the energy gap has been studied under conditions of atomic disorders [11]. A cubic phase of Mn_2FeSi has been synthesized using an annealing procedure [14]. It was obtained that Mn_2FeSi crystallizes in the inverse XA structure in contrast to Fe_2MnSi. In recent works [17,18] it is also reported, that Mn_2FeSi adopts a cubic inverse-Heusler structure. DFT-based calculations [15] showed that Mn_2FeSi in the inverse structure is a half-metal with a total magnetic moment of 2 μ_B. Thus, it is supposed that the Heusler

* Corresponding author.
E-mail address: jvc@iph.krasn.ru (V.S. Zhandun).

https://doi.org/10.1016/j.matchemphys.2021.124897
Received 14 February 2021; Received in revised form 5 June 2021; Accepted 28 June 2021
Available online 30 June 2021

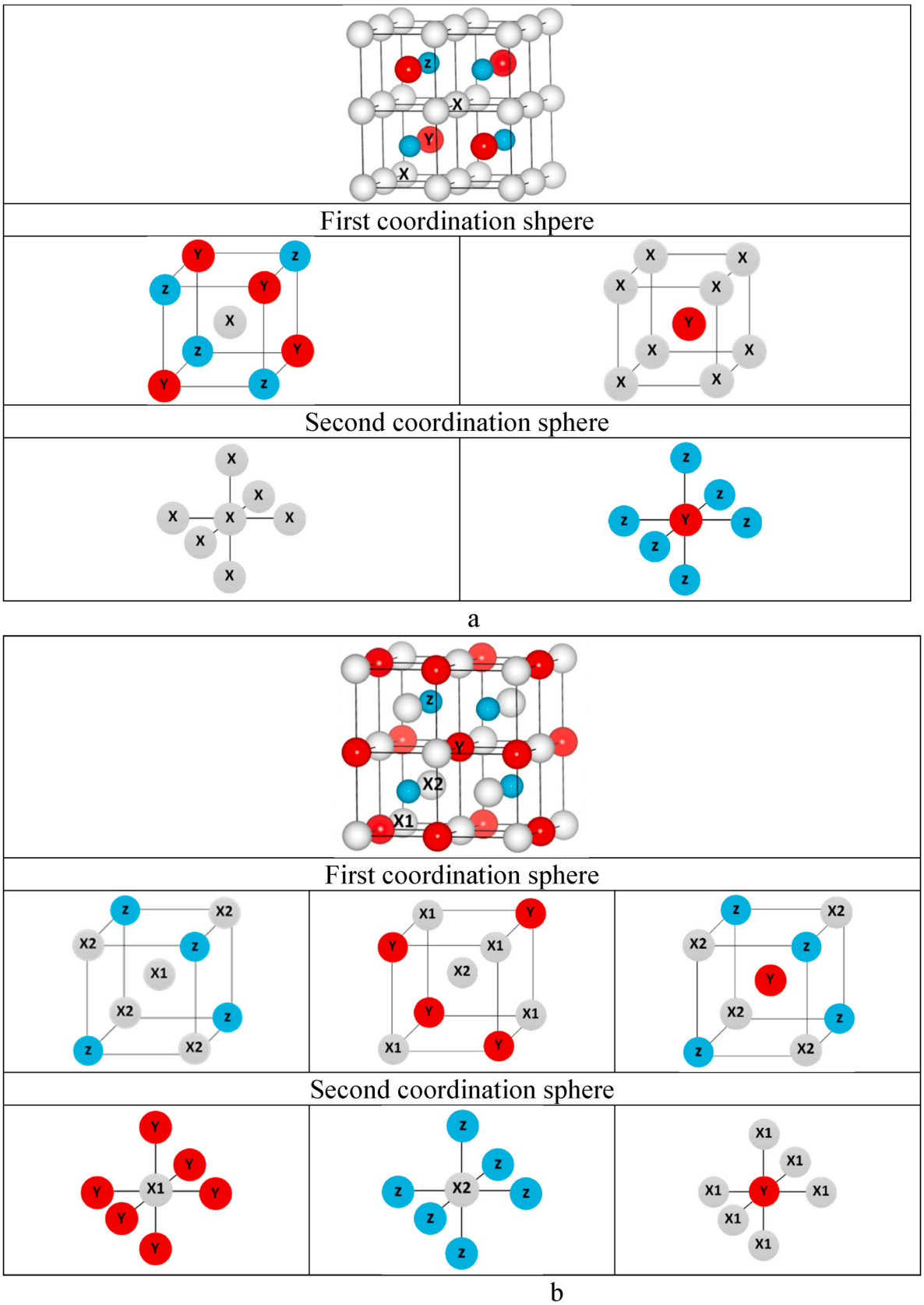

Fig. 1. Crystal structure and nearest and next-nearest local environment of Heusler compounds. a) Regular structure ($L2_1$) and b) inverse structure (XA).

Table 1
The lattice parameters a (Å) and the magnetic moments μ (μ_B) of transition metal atoms in Heusler alloys Fe_2MnSi and Mn_2FeSi in regular and inverse structures. The experimental values of the lattice parameter and previously calculated magnetic moments are given in parentheses. The last three columns show the difference in the total energies of the regular and inverse structures ΔE (eV/cell), formation enthalpy H_{cp} (eV/cell), and the type of the magnetic ordering.

Compound	A	A-site		B-site		C-site		ΔE	H_{cp}	Magnetic state
		atom	μ	atom	M	atom	μ			
Fe_2MnSi $L2_1$	5.52 (5.67 [7])	Fe	0.08 (0.01 [2])	Mn	2.83 (2.41 [2])	Fe	0.08 (0.01 [2])	0.00	−0.68	FM
Fe_2MnSi XA	5.58	Fe1	1.52	Fe2	2.57	Mn	−1.14	0.16	−0.44	FiM
Mn_2FeSi $L2_1$	5.54	Mn	−0.32	Fe	2.52	Mn	−0.32	0.62	−0.31	FM
Mn_2FeSi XA	5.59 (5.68 [10])	Mn1	−1.65 (−1.30 [12])	Mn2	2.92 3.00 [12]	Fe	0.78 (0.28 [12])	0.00	−0.48	FiM

compounds with transition metals can discover special properties such as half-metallicity as in the $L2_1$ structure as well in the XA structure depending on the chemical composition. Therefore it is of interest to compare the properties of some Heusler alloys in both regular and inverse structures. Existing studies provide insights into the beneficial properties and prospects of Mn_2FeSi and Fe_2MnSi Heusler alloys [2,11,18,19]. However, in such studies, only one of the possible structures of Heusler alloys was mainly considered. Here, we perform a comparative study of the properties of the Heusler compounds Mn_2FeSi and Fe_2MnSi of both regular ($L2_1$) and inverse (XA) structures to generalize and identify the features and mechanisms responsible for the formation of various structural, magnetic, and electronic properties observed in Heusler alloys. Moreover, in the present study, we aim to look at the properties of Heusler alloys from the point of view of the local environment and analyze its effect on the magnetic and electronic properties of the compounds.

The paper is organized as follows. In Sec. II, we give a short description of the computational details, in Sec. III.1 and III.2 the comparison of electronic and magnetic properties of the compounds in dependence of the composition and structure is given and analyzed. Sec. III.3 is devoted to the effect of the pressure on the electronic, magnetic, and structural properties. In the last Section, we make conclusions.

2. Calculation methods

Ab initio calculation of the electronic and magnetic properties has been performed within the framework of density functional theory (DFT) using the Vienna ab initio simulation package (VASP) [20,21] with a projector augmented wave (PAW) pseudopotentials [22]. The exchange-correlation functional was treated using GGA-PBE [23] and SCAN *meta*-GGA [24]. The valence electron configurations $3d^5 4s^2$ are taken for Mn atoms, $3d^6 4s^2$ for Fe atoms and $3s^2 3p^2$ for Si atoms. The Brillouin-zone integration is performed on the grid Monkhorst-Pack [25] special points $10 \times 10 \times 10$. Throughout all calculations, the plane-wave cutoff energy 500 eV is used. To calculate the formation enthalpy of the compounds we follow Ref. [26]. To include all competing phases, careful investigations of phase diagrams were carried out. A linear optimization procedure [27] was then used to identify the set of most competing phases for each Heusler alloys and the formation enthalpy Hcp for the identified most competing phases (cp) at zero pressure and temperature is calculated according to $H_{cp} = H[Heusler\ alloy] - H_{total}[cp]$. All phases were optimized with respect with cell volume, as well as internal parameters. Ferromagnetic as well as different antiferromagnetic structures were tested and the configuration with the lowest total energy was included in the study.

3. Results and discussion

3.1. Structural and magnetic properties

The full-Heusler compounds X_2YZ mainly have two possible structures: the regular structure of the Cu_2MnAl-type ($L2_1$) and the inverse structure of the Hg_2CuTi-type (XA). The atoms X and Y are transition metal d-elements and the atom Z is s- or p-element. The Wyckoff coordinates of non-equivalent positions for full-Heusler compounds are A (0, 0, 0), B (0.25, 0.25, 0.25), C (0.5, 0.5, 0.5) and D (0.75, 0.75, 0.75) (Fig. 1). Both structural types are described in detail in Ref. [28]. Here we want to emphasize the different local environments of transition metal atoms in these structures as shown in Fig. 1.

In the regular structure (Fig. 1a), X atoms (Fe for Fe_2MnSi and Mn for Mn_2FeSi, correspondingly) occupy equivalent A- and C positions and have 4 metal and 4 nonmetal atoms as nearest neighbors, while the next nearest neighbors in the second coordination sphere are only metal atoms X. Atom Y (Mn or Fe for Fe_2MnSi and Mn_2FeSi, correspondingly) occupies B-site and, vice versa, has a completely metallic environment in the first coordination sphere and only nonmetal atoms as next nearest neighbors.

In the inverse structure (Fig. 1b), the X atoms occupy the nonequivalent A- ($X1$) and B- ($X2$) sites, their nearest environment is significantly different. The local environment of the $X1$ atom is similar to the environment of the X atom in a regular structure, however, each metal atom has a different metal atom as next nearest neighbors: in Fe_2MnSi Mn atoms are surrounded by Fe1 and in Mn_2FeSi Fe atoms are surrounded by Mn1 atoms. The $X2$ atom is on B-site and has the same local environment as the Y atom in the regular structure. The Y atom in the inverse structure occupies the C-site and its local environment is the same as that of the $X1$ atom, i.e. has a completely metallic environment with metal atoms of a different type in the second coordination sphere and metal and non-metal atoms as nearest neighbors.

The different local environment of transition metal atoms leads to the pronounced difference between the magnetic moments' values of these atoms. Early we have performed the model analysis of the Mn_3Si и Fe_3Si Heusler compounds [29,30]. It was shown that the magnetic state of the Heusler compounds mainly depends on the location of the metal atoms in the local environment. Calculated magnetic phase diagrams [29,30] show the presence of the sharp boundary between magnetic and nonmagnetic states, at that the magnetic state of the compounds is near a boundary. As shown in Ref. [30], such the sharp boundary between the magnetic states appears due to the couplings between metal atoms within the second coordination sphere. It is this coupling is responsible for the magnitude of the magnetic moment of the corresponding atom. The presence of the metal atoms as the next-nearest neighbors of the transition metal atom leads to the forming of the strong σ-bonds between d-electrons of these atoms. In this case, a delocalization of d-electrons and a decrease in the magnetic moment are observed. As emphasized in Refs. [29,30], this feature, is common for Heusler compounds. In the studied compounds such a metallic environment in the second coordination sphere is observed for atoms occupying A- and C-sites (Fig. 1). At the same time, the metal atoms located at the B-site have metal atoms only as nearest neighbors. Thus, according to the conclusions of Refs [29,30], the atoms on the A- and C-sites should have a small magnetic moment, while the atom on the B-site should have a large one. The results of our calculations of the magnetic moments of Fe_2MnSi and Mn_2FeSi Heusler alloys confirm this conclusion.

The SCAN-based equilibrium lattice parameters and magnetic moments of Fe_2MnSi and Mn_2FeSi in both regular and inverse structures are given in Table 1. As shown, Fe_2MnSi and Mn_2FeSi are realized in different structures. The regular structure is the most favorable for

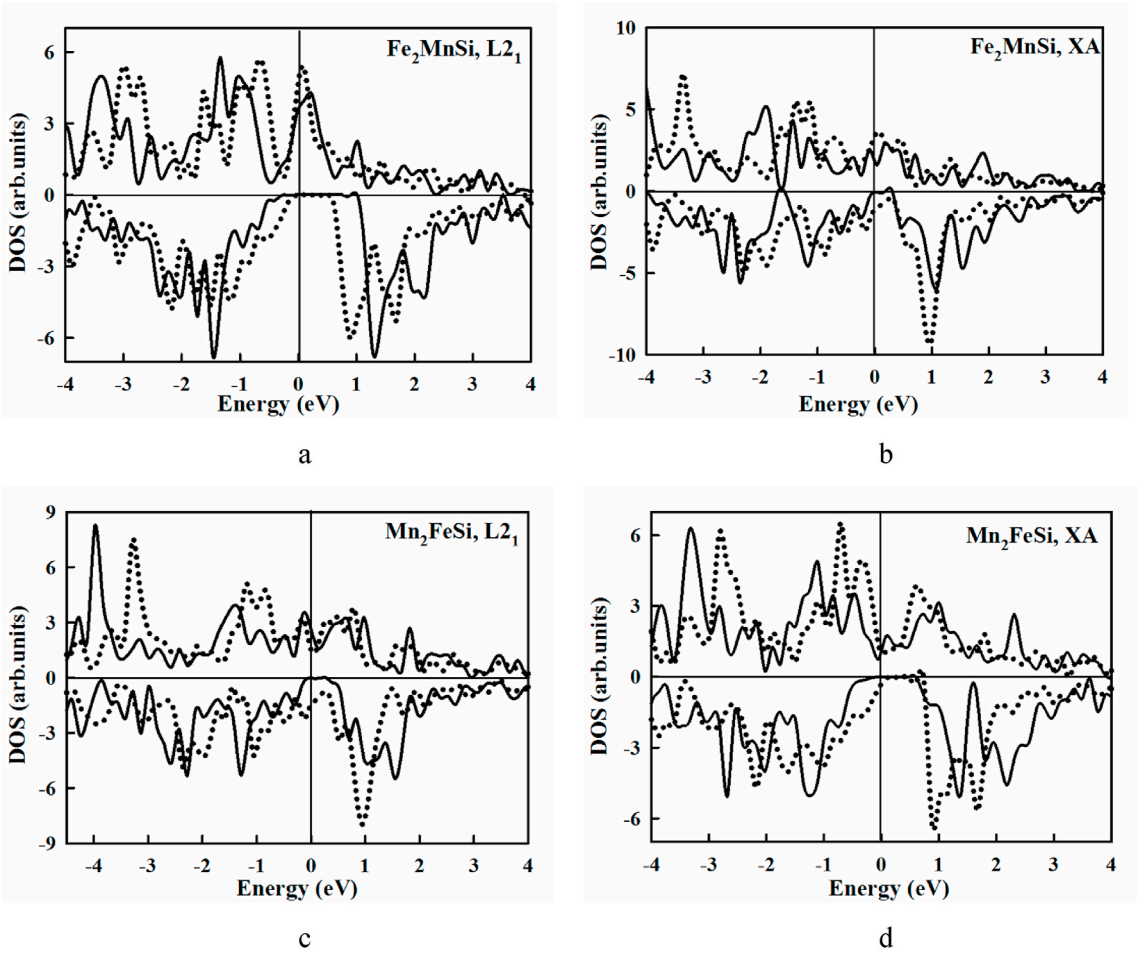

Fig. 2. The total density of states for Fe_2MnSi in regular (a) and inverse (b) structures; the total density of states for Mn_2FeSi in regular (c) and inverse (d) structures. Solid line – SCAN-based results, dotted line – GGA. Zero on the energy axis corresponds to the Fermi energy.

Fe_2MnSi, while in Mn_2FeSi the inverse structure is lower by energy (Table 1, 9th column). This is agreed with the known experimental data [11,14]. The values of equilibrium lattice parameters are very close regardless of the chemical composition and structure. As can be seen from the last column of Table 1, in regular structure Fe_2MnSi and Mn_2FeSi are ferromagnetics (FM), and they are ferrimagnetic (FiM) in the inverse structure. In both structural types, the B-site atom has a large magnetic moment, while the A- and *C*-sites atoms have smaller ones. SCAN-based calculation demonstrates higher values of magnetic moments compared to GGA. Notice, the present magnetic moments are close to ones obtained from other calculations [2,16].

Thus, the assumptions in Refs. [29,30] about the effect of the local environment on the magnitude of the magnetic moment are also confirmed here for Heusler alloys Fe_2MnSi and Mn_2FeSi.

3.2. The electronic structure

Fig. 2 shows the total densities of states (DOS) of Mn_2FeSi and Fe_2MnSi compounds in the regular and inverse structures, calculated within GGA (dotted line in Fig. 2) and SCAN (solid line in Fig. 2) approximations. As is known, the GGA approximation inaccurately estimates the energy bandgap, significantly underestimating its value. In both approximations, inverse Mn_2FeSi compound and regular Fe_2MnSi compound are half-metals with the energy bandgap for the minority spin states (Fig. 2d, a). However, SCAN increases the bandgap from ~0.8 eV (within GGA) to ~ 1.1 eV for regular Fe_2MnSi (Fig. 2a) and from ~0.5 eV (within GGA) to ~ 1.0 eV for inverse Mn_2FeSi (Fig. 2d). The values of the bandgap obtained here for both compounds are in good agreement with the results of other calculations obtained within the GGA + U approximation [31,32] For example, in Refs. [31,32] the bandgap was obtained as ~ 0.9 eV [31] and ~1.0 eV [32] for regular Fe_2MnSi. The high spin polarization of these compounds is agreed with the other calculations [2,16]. In turn, Mn_2FeSi in regular structure (Fig. 2c) and Fe_2MnSi in inverse structure (Fig. 2b) are metals within GGA, whereas SCAN–based calculations result in the appearance of the small bandgap ~0.2eV–0.4eV (Fig. 2c,b). Since SCAN has shown to be very successful in describing electronic properties, such as band structure and DOS, especially for the systems with strong electron correlations, we will perform further investigation within SCAN-based results.

Fig. 3 shows the partial density of states of d-electrons for Fe_2MnSi and Mn_2FeSi in regular and inverse structures. All projected DOS have pronounced peaks, corresponding to the strong localization of the B-site atoms' electrons. As seen, the appearance of the half-metallic properties in these Heusler compounds is mainly related to the behavior of the t_{2g} electrons of the transition metal atoms. The delocalization of these electrons results in the strong decrease of the half-metallic bandgap in the regular Mn_2FeSi compound and the inverse Fe_2MnSi compound (Fig. 3). To some extent, it is related to the interaction of the nearest metal atoms (Fig. 1). Next, we consider the projected DOS of minority spin state t_{2g}-electrons of the transition metals in more detail.

Let us consider the regular Fe_2MnSi and Mn_2FeSi compounds (Fig. 2a,c Fig. 3a,b,e,f). Mn atom in the regular Fe_2MnSi and Fe atom in regular Mn_2FeSi occupy B-site and have a large magnetic moment. At that, these atoms have differences in the local environment: Mn atom in regular Fe_2MnSi has four Fe atoms as nearest neighbors, whereas Fe atom in regular Mn_2FeSi has four Mn atoms as nearest neighbors (Fig. 1).

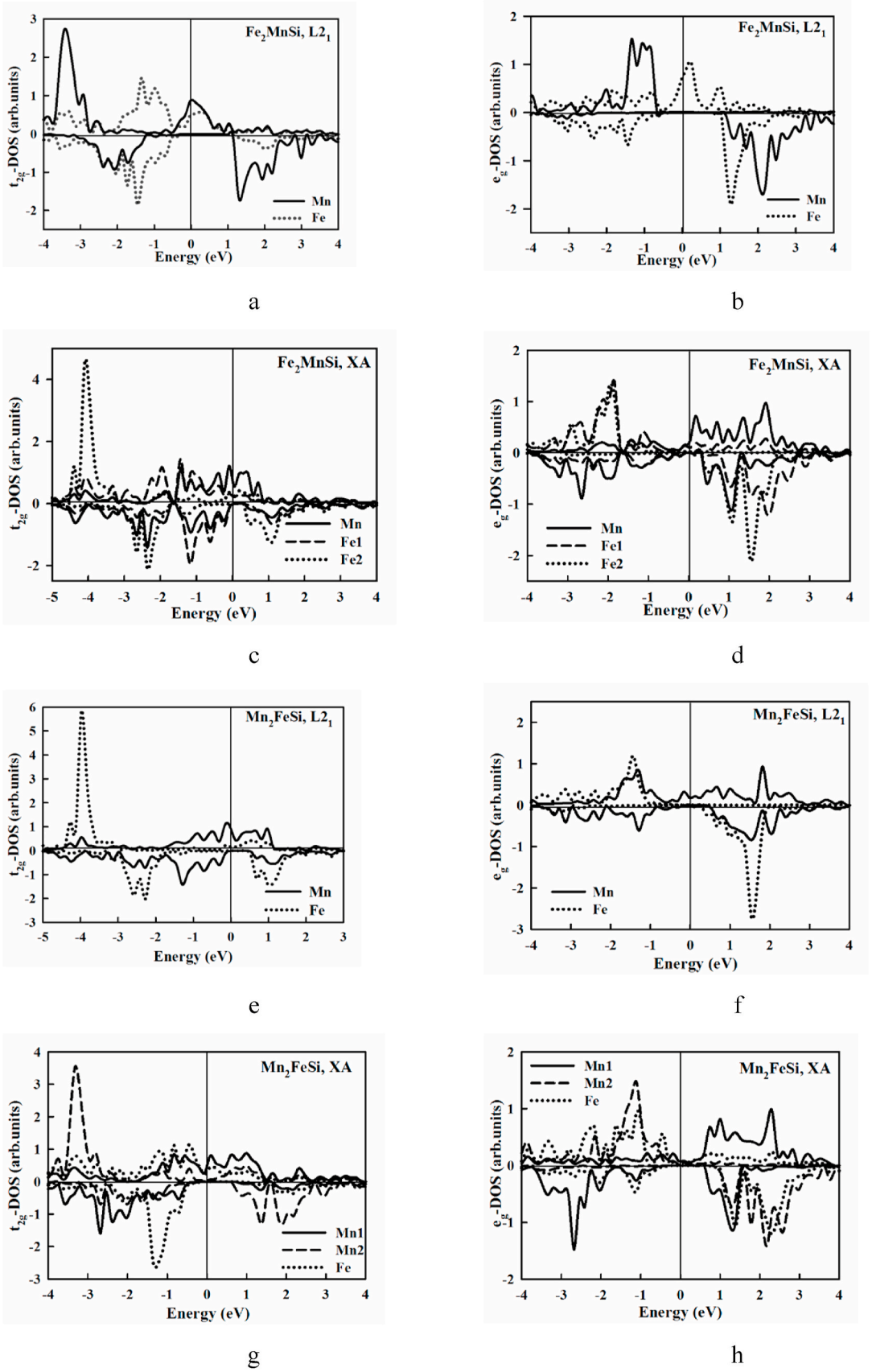

Fig. 3. The partial density of states of d-electrons for Fe_2MnSi in regular structure (a, b) Fe_2MnSi in inverse one (c, d), Mn_2FeSi in regular structure (e, f) and Mn_2FeSi in inverse one (g, h). Zero on the energy axis corresponds to the Fermi energy.

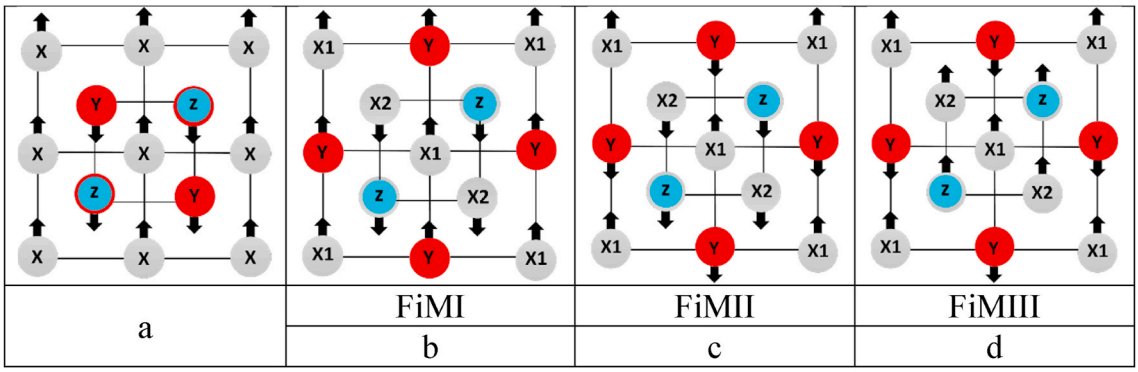

Fig. 4. The types of the magnetic orderings for regular structure (a) and inverse structure (b, c, d).

This difference in the local environment leads to the difference in the densities of electronic states, namely, in regular Mn_2FeSi t_{2g}-electrons of Mn atoms are delocalized in a wider energy range than t_{2g}-electrons of Fe atoms in the regular Fe_2MnSi. As a result, a half-metal bandgap significantly decreases in the regular Mn_2FeSi as compared with the regular Fe_2MnSi.

In inverse structures (Fig. 2b, d, Fig. 3c, d, g, h), the situation is more complicated, since the X atoms occupy nonequivalent B- and A-sites. Accordingly, in the inverse Fe_2MnSi (Fig. 3c and d) the B-site is occupied by one of the iron atoms (Fe2) and in the inverse Mn_2FeSi compound, B-site is occupied by one of the manganese atoms (Mn2) (Fig. 3g and h). In the inverse Fe_2MnSi, two regions of strong hybridization of transition metal t_{2g}-electrons can be distinguished (Fig. 3c). The first one, at lower energies (-3eV; -2eV), is related to the hybridization of Mn and Fe1 t_{2g}-electrons interacting with each other in the second coordination sphere. The second region at higher energies (−1.5eV–0eV) corresponds to the hybridization of Mn and Fe2 t_{2g}-electrons interacting with each other in the first coordination sphere. It is this interaction that contributes to a significant decrease in the energy bandgap in the t_{2g} minority spin channel in inverse Fe_2MnSi. In inverse Mn_2FeSi (Fig. 3g), the situation is somewhat different. The local environment of the Fe atom in the first coordination sphere is here the same as in the regular Mn_2FeSi compound: the Fe atom has four Mn atoms as nearest neighbors. And, as in the regular Mn_2FeSi compound, the t_{2g}-electrons of Mn atoms are delocalized in a wide energy range. The shift of the delocalization area of t_{2g}-electrons towards lower energies decreases minority spin bandgap and is related to the strong hybridization of the t_{2g}-electrons of manganese atoms. Manganese atoms Mn1 and Mn2 interact only in the first coordination sphere, but at the same time, the B-site atom (Mn2) has only nonmetal Z atoms as the next-nearest neighbors. Therefore, Mn2 electrons are localized at energies of ∼ −3.5 eV and hybridization of Mn1 and Mn2 t^{2g} -electrons are observed in the energy range (-3eV - -1eV).

Thus, the local environment plays a crucial role in the appearance of half-metallicity in Heusler alloys under consideration. We can see that bonds that arise between the nearest metal atoms are responsible for the appearance of a half-metallic bandgap. Since the nearest metal-metal neighbors are along (111) direction in the corner of the cube (Fig. 1), then the formation of the bonds is mainly related to the overlap of the t_{2g}-orbitals of the transition metal atoms. Also, it should be noted that a significant half-metal bandgap appears only when the B-site is occupied by the Mn atom with a large magnetic moment. If the B-site is occupied by an iron atom, then the energy gap in the minority spin state significantly decreases. This feature was also observed in other Heusler alloys with a similar composition, for example, Mn_3Si is a half-metal, while Fe_3Si is not [29,30].

3.3. *Effect of the pressure*

Let us consider the effect of the pressure on the electronic, magnetic and structural properties. The pressure dependence of the enthalpy and electronic and magnetic properties were studied at the different initial magnetic configurations by changing lattice parameters from a = 5.0 A to a = 6.5 A that corresponds to the pressure range from 150 GPa to −25 GPa.

Since the magnetic configurations can be changed under pressure, we have used different initial magnetic configurations to check all possible cases (Fig. 4): (FM) - ferromagnetic, (FiMI) - antiferromagnetic, where the moments on the A- and *C*- site atoms are co-directed, (FiMII) - antiferromagnetic, where the moments on the B-, and *C*-site atoms are co-directed, (FiMIII) - antiferromagnetic, where the moments are co-directed on A- and B-site atoms When all compounds are compressed up to 150 GPa, no peculiarities were observed in the behavior of the magnetic moment and enthalpy as a function of pressure. The regular structure compounds prefer the ferromagnetic (FM) configuration in Fe_2MnSi and ferrimagnetic one (FiMI) in Mn_2FeSi, while compounds with the inverse structure prefer the antiferromagnetic (FiMIII in Fe_2MnSi and FiMII in Mn_2FeSi) configurations. Regardless of the choice of the initial magnetic configuration, the magnetic moments of the atoms monotonically tend to zero under the compressive pressure. Similar behavior is observed for Mn_2FeAl and Fe_2MnAl also in Ref. [5], where the collapses of a magnetic moment have been detected in both alloys at 450 GPa and 175 GPa, correspondingly. Besides, the half-metallic properties were found to be retained up to 80 GPa in regular Fe_2MnSi and throughout the studied pressure range in inverse Mn_2FeSi.

Another situation was observed under tensile pressure, that is, at negative pressures: pressure dependence of the magnetic moments has obvious features. At that, the behavior of the magnetic moments depends on the initial magnetic configuration. Therefore, the most energetically favorable magnetic configuration was determined by comparing the enthalpies of various magnetic phases under pressure. For each pressure point, exactly the magnetic configuration was taken that had the lowest enthalpy at a given pressure. The dependence of the magnetic moment on pressure is shown in Fig. 5 in the pressure range from 0 GPa to −20 GPa since it is in this range that features in the dependence of magnetic properties on pressure are observed.

Let us consider the half-metal regular Fe_2MnSi compound (Fig. 5a). Regardless of the initial magnetic configuration, the compounds remain ferromagnetic down to the pressure P = -14 GPa. At a pressure of about −14 GPa, a magnetic transition from a ferromagnetic phase to the FiMI phase is observed. As a result, there is a sharp change in the magnitude of the magnetic moment on A- and *C*-site atoms in this pressure range, while the magnetic moment of the B-site atom changes less. Moreover, at the pressure of about −3 GPa the compound loses the half-metallicity, and the minority spin bandgap close. Fig. 6a shows a comparison of

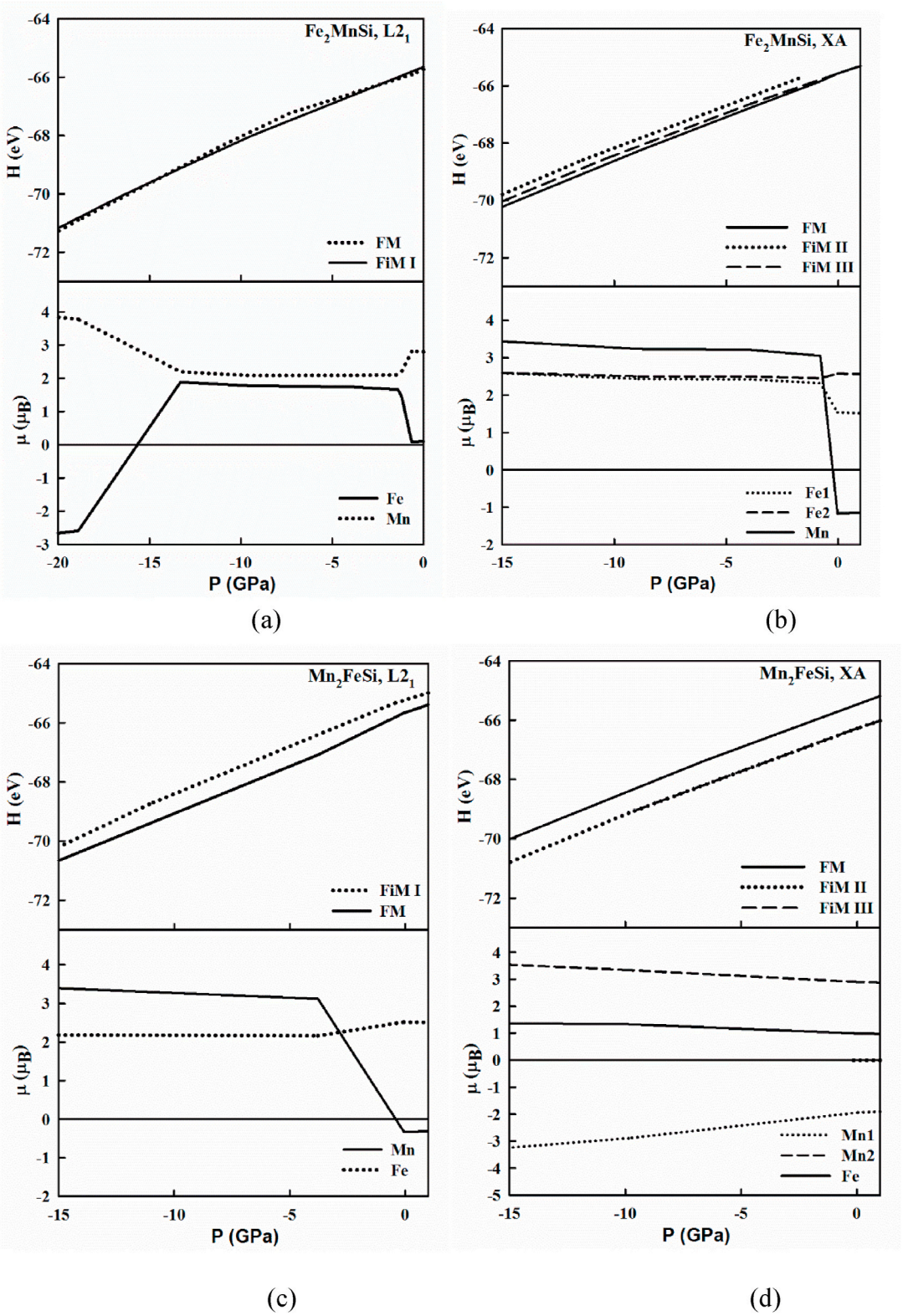

Fig. 5. The pressure dependence of the enthalpy and the magnetic moments of (a) regular Fe_2MnSi (The vertical dashed line shows the transition between different magnetic phases), (b) inverse Fe_2MnSi, (c) regular Mn_2FeSi, (d) inverse Mn_2FeSi.

the total DOS in the absence of external pressure and under a pressure of −13 GPa, at which there is no energy bandgap for minority spin states. As can be seen, the pressure shifts the density of states up to the Fermi level in such a way that the minority spin t_{2g} states of the iron atom at the A- and *C*- sites fall on the Fermi energy, closing the energy gap. The DOS peaks become more pronounced since electrons become more localized with increasing distances between atoms.

The inverse Fe_2MnSi compound is a half-metal with a minority spin bandgap. The compound has FiMII magnetic configuration with a small negative magnetic moment on the Mn atom in the *C*-site (Fig. 5b). At a

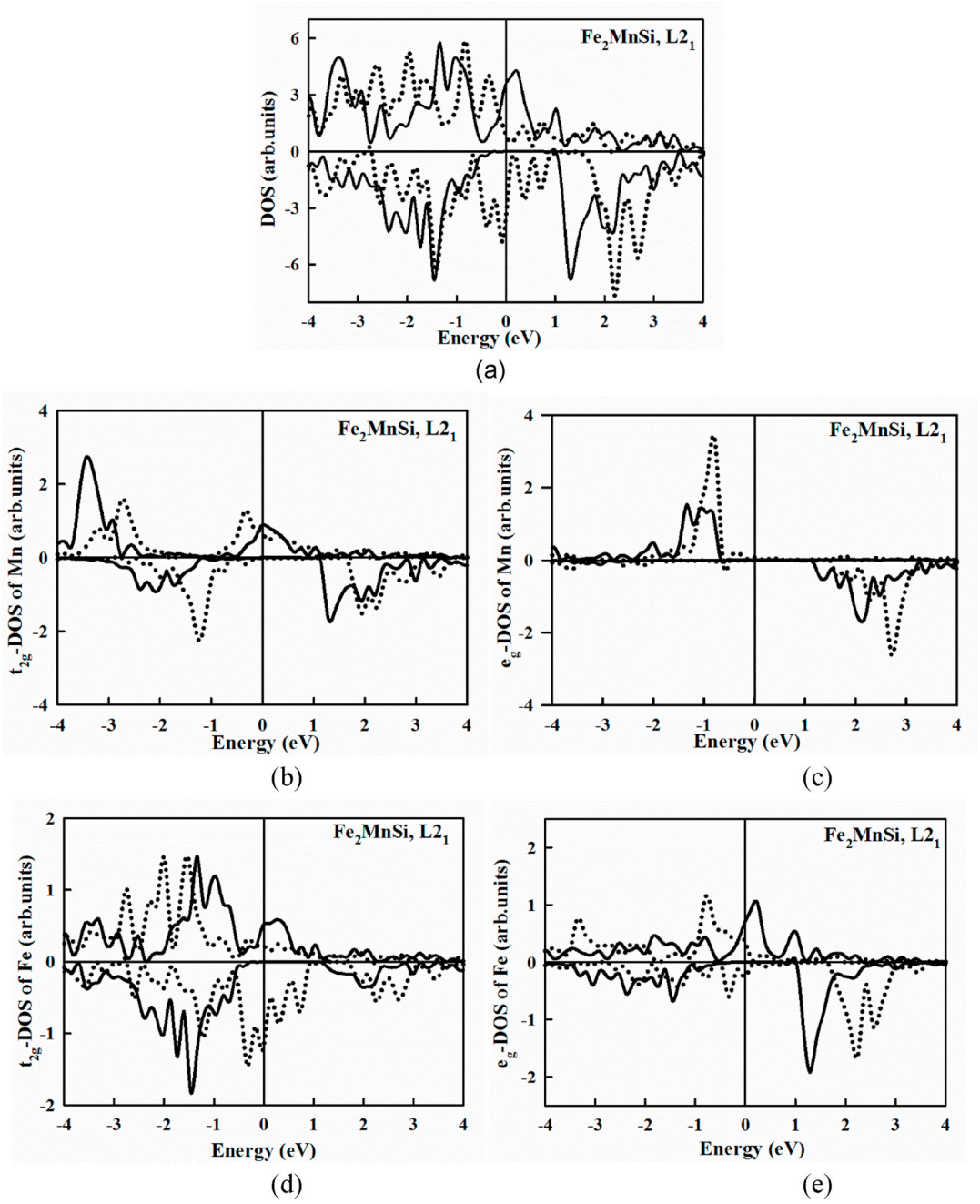

Fig. 6. (a) The comparison of the total DOS of Fe_2MnSi at zero pressure and under the pressure of −24 GPa; the partial densities of states for (b) t_{2g} states of Fe (A,C) (c) e_g states of Fe (A,C) (d) t_{2g} states of Mn (B) (e) e_g states of Mn (B). DOS at zero pressure is shown by dashed line and DOS under the pressure of −24 GPa is shown by the solid line. Zero on the energy axis corresponds to the Fermi energy.

pressure of −1 GPa, the compound becomes ferromagnetic. There is a sharp increase in the magnetic moments of atoms at Fe1 and Mn, on A- and *C*- sites, correspondingly.

Regular Mn_2FeSi is also half-metal with a small minority spin as the inverse Fe_2MnSi compound and has the same behavior under pressure. It is ferrimagnetic (FiMI) with small negative magnetic moments on the Mn atoms in A- and *C*- sites, however, at the pressure of −3 GPa the ferromagnetic state becomes the most favorable by the energy (Fig. 5c). At this pressure, a sharp increase in the magnetic moments on manganese atoms (A- and *C*- sites) is observed, while the magnetic moment on iron atoms (B-site) does not change under tensile pressure.

Finally, we have considered the inverse Mn_2FeSi (Fig. 5d). When the crystal is under tensile pressure, the compound prefers FiMIII magnetic configuration. The absolute value of the magnetic moments on all atoms smoothly increases with increasing pressure. In this compound, the half-metallic minority spin bandgap remains up to a pressure of −9 GPa. The width of the bandgap for minority spin states decreases and tends to zero under pressure.

Thus, there are common features observed for all compounds when negative pressure was applied. i) The magnetic moments on the B-site atoms smoothly increase from 2 μB to 3.5 μB throughout the entire negative pressure range (Fig. 5). ii) In contrast, the magnetic moments on A- and *C*-site atoms change more dramatically under pressure. At zero pressure, the magnetic moments on the A- and *C*-site atoms are small and abruptly increase under tensile pressure (Fig. 5). This is due to a sharp change in the occupation numbers of d-orbitals, especially t_{2g}-

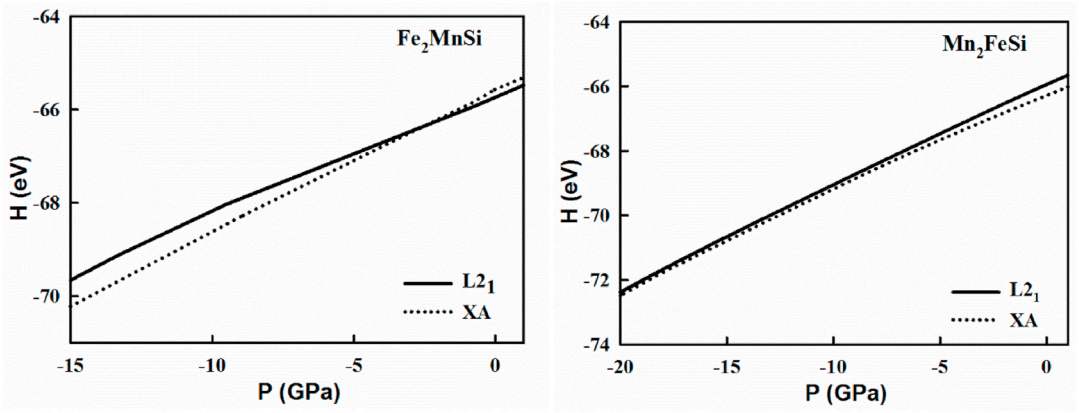

Fig. 7. The pressure dependence of enthalpy for (a) Fe_2MnSi, (b) Mn_2FeSi. Dashed line corresponds to the regular structure and solid line corresponds to inverse one.

orbitals for minority spin states at critical pressure. At a pressure of −16 GPa, the occupation numbers of atoms of minority spin orbitals decrease abruptly, while the occupation numbers of majority spin orbitals increase abruptly. Moreover, a sharp increase in the occupation number of minority spin t_{2g} orbitals corresponds to a shift of the corresponding peak of t_{2g}-electrons to the Fermi level (Fig. 6) that leads to the closure of the energy bandgap and the disappearance of half-metallicity at a given pressure. At that, the pressure dependence of the occupation numbers of the A-,C- site atom is much less pronounced.

At last, we would like to note that negative pressure also leads to a transition between regular and inverse structures (Fig. 7). So, the regular structure of Fe_2MnSi is more favorable by energy up to −2 GPa, while the increase of the pressure leads to the inverse structure becomes more favorable. However, in Mn_2FeSi inverse structure remains more favorable up to −25GPa.

It is in the range from 0 GPa to −3 GPa (i.e., near the transition point), the magnetic moments in the regular Fe_2MnSi undergo abrupt change (Fig. 5). The structural transition between regular and inverse structures requires the displacement of two atoms in the crystal lattice, which is difficult to implement in practice. But the growth of compounds under a certain pressure to obtain the desired structure and magnetic properties is possible [33].

4. Conclusions

In summary, we have studied how the electronic and magnetic properties depend on the structure, composition, and pressure in the Mn_2FeSi and Fe_2MnSi Heusler alloys. The effect of the local environment and the dependence of the electronic and magnetic properties on the composition and structure were analyzed. We have shown that the half-metal minority spin bandgap is related to the hybridization of t_{2g}-electrons of A- and *C*-sites atoms. Hybridization arises due to the overlap of the t_{2g}-orbitals of transition metal atoms located along the [111] direction and forming the first coordination sphere. The magnetic moment of the B-site atoms is much larger than the magnetic moments of A- and *C*-site atoms due to the differences in the local environment of B- and A-, *C*-site atoms. At that, the magnetic moment of B-site atoms is less sensitive to the pressure than magnetic moments of A- and *C*- site atoms. The strong sensitivity of the A- and C-site magnetic moments to pressure leads to their abrupt increase under tensile pressure. The pressure leads to the sharp electron transfer from minority spin states to the majority spin states on these atoms and the sharp increase of magnetic moment. This pressure-dependent electron transfer also results in the close of the minority spin state bandgap in the inverse Mn_2FeSi and regular Fe_2MnSi and the disappearance of the half-metallicity under tensile pressure. At last, we have predicted the transition of studied compounds from regular to the inverse structure under the negative pressure.

CRediT authorship contribution statement

Oksana N. Draganyuk: Software, Investigation, Writing – original draft. **Vyacheslav S. Zhandun:** Methodology, Validation, Software, Investigation, Data curation, Formal analysis, Writing – review & editing. **Natalia G. Zamkova:** Software, Investigation, Conceptualization, Methodology, Validation, Formal analysis, Writing – review & editing, Supervision.

Declaration of competing interest

The authors declare that they have no known competing financial interests or personal relationships that could have appeared to influence the work reported in this paper.

Acknowledgments

The reported study was funded by Russian Foundation for Basic Research, Government of Krasnoyarsk Territory, Krasnoyarsk Regional Fund of Science to the research projects No19-42-240016: «Control of structural, magnetic, electronic, and optical properties by pressure and intercalation into functional compounds with a spinel structure containing 3 d and 4f ions» and 20-42-240004: "The effect of the composition, pressure, and dimension on the magnetic, electronic, optical, and elastic properties of the magnetic $M_{n+1}AX_n$ (M = Cr, Mn; Fe, A = Al, Ga, Si, Ge, P, In; X = C, N; n = 1–3) MAX-phases". The calculations were performed with the computer resources of "Complex modeling and data processing research installations of mega-class" SRC "Kurchatovsky Institute" (http://ckp.urcki.ru).

References

[1] M.N. Rasul, A. Javed, M.A. Khan, A. Hussain, Structural stability, mechanical, electronic and magnetic behavior of quaternary ScNiCrX (X = Al, Ga) Heusler alloys under pressure, Mater. Chem. Phys. 222 (2018) 321–332, https://doi.org/10.1016/j.matchemphys.2018.09.015.

[2] M. Belkhouane, S. Amari, Yakoubi, et al., First-principles study of the electronic and magnetic properties of Fe_2MnAl, Fe_2MnSi and $Fe_2MnSi_{0.5}Al_{0.5}$, J. Magn. Magn Mater. 377 (2015) 211–214, https://doi.org/10.1016/j.jmmm.2014.10.094.

[3] A. Abada, K. Amara, S. Hiadsi, B. Amrani, First principles study of a new half-metallic ferrimagnets Mn2-based full Heusler compounds: Mn2ZrSi and Mn2ZrGe, J. Magn. Magn Mater. 388 (2015) 59–67, https://doi.org/10.1016/j.jmmm.2015.04.023.

[4] P.O. Adebambo, B.I. Adetunji, Olowofela, et al., Prediction of metallic and half-metallic structure and elastic properties of Fe2Ti1−xMnxAl Heusler alloys, Phys. B

Condens. Matter 485 (2016) 103–109, https://doi.org/10.1016/j.physb.2016.01.014.
[5] Y. Ze-Jin, G. Qing-He, X. Heng-Na, et al., Pressure-induced magnetic moment abnormal increase in Mn2FeAl and non-continuing decrease in Fe2MnAl via first principles, Sci. Rep. 7 (1) (2017) 16522, https://doi.org/10.1038/s41598-017-16735-1.
[6] S. Qi, C.-H. Zhang, B. Chen, J. Shen, N. Chen, First-principles study on the ferrimagnetic half-metallic Mn2FeAs alloy, J. Solid State Chem. 225 (2015) 8–12, https://doi.org/10.1016/j.jssc.2014.11.026.
[7] S. Ahmad Khandy, J.-D. Chai, Novel half-metallic L21 structured full-Heusler compound for promising spintronic applications: a DFT-based computer simulation, J. Magn. Magn Mater. (2019) 165289, https://doi.org/10.1016/j.jmmm.2019.165289.
[8] S. Ahmad Khandy, Jeng-da chai, J. Phys. Chem. Solid. 154 (2021) 110098, https://doi.org/10.1016/j.jpcs.2021.110098.
[9] S. Ahmad Khandy, Jeng-da chai, J. Alloys Compd. 850 (2021) 156615, https://doi.org/10.1016/j.jallcom.2020.156615.
[10] S. Ahmad Khandy, I. Islam, D.C. Gupta, R. Khenata, A. Laref, Sci. Rep. 9 (2019) 1475, https://doi.org/10.1038/s41598-018-37740-y.
[11] N.I. Kourov, V.V. Marchenkov, Korolev, et al., Specific features of the properties of half-metallic ferromagnetic Heusler alloys Fe2MnAl, Fe2MnSi, and Co2MnAl, Phys. Solid State 57 (4) (2015) 700–708, https://doi.org/10.1134/s1063783415040149.
[12] A. Vinesh, H. Bhargava, N. Lakshmi, K. Venugopalan, Magnetic anisotropy induced by high energy ball milling of Fe2MnAl, J. Appl. Phys. 105 (7) (2009), 07A309, https://doi.org/10.1063/1.3063676.
[13] C. Paduani, A. Migliavacca, Pöttker, et al., A study of alloys: structural and magnetic properties, Phys. B Condens. Matter 398 (1) (2007) 60–64, https://doi.org/10.1016/j.physb.2007.04.068.
[14] Said Bakkar, New Inverse-Heusler Materials with Potential Spintronics Applications Theses. 2207, Southern Illinois University Carbondale, United States, 2017, p. 75p.
[15] S.V. Faleev, Y. Ferrante, J. Jeong, M.G. Samant, B. Jones, Parkin, Phys. Rev. 7 (3) (2017), https://doi.org/10.1103/PhysRevApplied.7.034022.
[16] H.Z. Luo, H.W. Zhang, Zhu, et al., J. Appl. Phys. 103 (8) (2008), 0839908, https://doi.org/10.1063/1.2903057.
[17] Jianhua Ma, Jiangang He, Dipanjan Mazumdar, et al., Phys. Rev. B 98 (2018), 094410, https://doi.org/10.1103/PhysRevB.98.094410.
[18] A. Aryal, S. Bakkar, H. Samassekou, et al., Mn2FeSi: an antiferromagnetic inverse-Heusler alloy, J. Alloys Compd. 823 (2020) 153770, https://doi.org/10.1016/j.jallcom.2020.153770.
[19] A.B. Granovskii, E.A. Soboleva, Fadeev, et al., Martensitic phase transition in magnetic thin films based on inverse Mn2FeSi heusler alloys, J. Exp. Theor. Phys. 130 (1) (2020) 117–122, https://doi.org/10.1134/s1063776119120033.
[20] G. Kresse, J. Furthmuller, Efficiency of ab-initio total energy calculations for metals and semiconductors using a plane-wave basis set, Comput. Mater. Sci. 6 (1996) 15.
[21] G. Kresse, J. Furthmuller, Efficient iterative schemes for ab initio total-energy calculations using a plane-wave basis set, Phys. Rev. B 54 (1996) 11169.
[22] P.E. Blochl, Projector augmented-wave method, Phys. Rev. B 50 (1994) 17953.
[23] J.P. Perdew, K. Burke, M. Ernzerhof, Generalized gradient approximation made simple, Phys. Rev. Lett. 77 (1997) 3865.
[24] J. Sun, A. Ruzsinszky, J.P. Perdew, Phys. Rev. Lett. 115 (2015), 036402.
[25] H.J. Monkhorst, J.D. Pack, Special points for Brillouin-zone integrations, Phys. Rev. B 13 (1976) 5188.
[26] M. Dahlqvist, B. Alling, J. Rosen, Phys. Rev. B81 (2010), 220102(R).
[27] M. Dahlqvist, J. Rosen, The Royal Society of Chemistry Nanoscale 12 (2020) 785–794.
[28] T. Graf, C. Felser, S.S.P. Parkin, Simple rules for the understanding of Heusler compounds, Prog. Solid State Chem. 39 (1) (2011) 1–50, https://doi.org/10.1016/j.progsolidstchem.2011.02.001.
[29] N.G. Zamkova, V.S. Zhandun, S.G. Ovchinnikov, I.S. Sandalov, Effect of local environment on moment formation in iron silicides, J. Alloys Compd. 695 (2017) 1213–1222.
[30] O.N. Draganyuk, V.S. Zhandun, N.G. Zamkova, Effect of the local environment on the magnetic properties of Mn3Si: hybrid ab initio and model study, Phys. Status Solidi 256 (12) (2019) 1900228, https://doi.org/10.1002/pssb.201900228.
[31] Y. El Krimia, R. Masroura, A. Jabara, S. Labidib, M. Bououdinac, M. Ellouzed, Results in Physics 18 (2020) 103252.
[32] Sonu Sharma, K. Sudhir, Pandey, Journal of Magnetism and Magnetic Materials 403 (2016) 1–7.
[33] Hongzhi Luo, Wei Zhu, Li Ma, Guodong Liu, Yangxian Li, Xiaoxi Zhu, Chengbao Jiang, Huibin Xu, Guangheng Wu, J. Phys. D Appl. Phys. 42 (2009), 095001.